Eclipsing binaries in the Galactic Bulge: candidates for distance estimates *

M.A.T. Groenewegen

Instituut voor Sterrenkunde, K.U. Leuven, PACS-ICC, Celestijnenlaan 200B, B-3001 Leuven, Belgium

received: 2005, accepted: May 4th, 2005

Abstract. The 222 000 I-band light curves of variable stars detected by the OGLE-II survey in the direction of the Galactic Bulge have been searched for eclipsing binaries (EBs). A previously developed code to analyze lightcurve shapes and identify long period variables (LPVs) has been adapted to identify EBs. The parameters in the modified code have been optimised to recover a list of about 140 detached EBs in the Small Magellanic Cloud previously identified in the literature as particularly well suited for distance estimates (and wich have periods \gtrsim 0.85 days). The power of the code is demonstrated by identifying 16 and 178 previously uncatalogued EBs in the SMC and LMC, respectively. Among the 222 000 variable stars in the direction of the Galactic Bulge 3053 EBs have been identified. Periods and phased lightcurves are presented.

Key words. Stars: distances - binaries: eclipsing - Galaxy: bulge - distance scale

1. Introduction

Detached double-lined eclipsing binaries (hereafter EBs for short) are very suitable as primary distance indicators when accurate photometry and radial velocity (RV) data are combined (e.g. Andersen 1991). The massive photometric monitoring data obtained in the course of the micro lensing surveys in the 1990's of the Small and Large Magellanic Clouds has revealed many candidate detached eclipsing binaries based on the shape of the lightcurves (Grison et al. 1995, Alcock et al. 1997, Udalski et al. 1998, Bayne et al. 2002, Wyrzykowski et al. 2003, 2004).

Some of them have been followed-up with spectroscopy to obtain RV data and perform a combined lightcurve and RV curve analysis to obtain the distance to the system (see e.g., Guinan et al. 1998, Hilditch et al. 2005, and the review by Clausen 2004 for a list of systems with recent distance estimates). What makes EBs particularly powerful is that the error in the distance estimate in a single well-observed system (0.06 - 0.10 in distance modulus, see Clausen 2004) is already comparable to the dispersion in optical and infrared Cepheid PL-relation based on hundreds of stars (e.g. Sandage et al. 2004, Nikolaev et al. 2003).

In the present paper a list of eclipsing binaries in the direction of the Galactic Bulge (GB) is presented based on analysis of OGLE-II data. Previously, 1650 EBs have been identified in OGLE-I data (Udalski et al. 1994, 1995a, 1995b, 1996, 1997).

The paper is structured as follows. In Section 2 the OGLE-II surveys is briefly described. In Section 3 the model to identify EBs from the lightcurve shape is briefly presented. The results are presented in Section 4, and discussed in Section 5.

2. The data sets

The OGLE-II micro lensing experiment observed fourty-nine fields in the direction of the GB. Each field has a size $14.2' \times 57'$ and was observed in BVI, with an absolute photometric accuracy of 0.01-0.02 mag (Udalski et al. 2002). Table 1 lists the galactic coordinates of the field centers and the total number of sources detected in these fields.

Wozniak et al. (2002) present a catalog of about 222 000 variable objects based on the OGLE observations covering 1997-1999, applying the difference image analysis (DIA) technique on the I-band data. The data files containing the I-band data of the candidate variable stars was downloaded from the OGLE homepage (http://sirius.astrouw.edu.pl/ \sim ogle/).

3. Analysis of the lightcurve shape and selecting eclipsing binaries

The model to analyse the lightcurve shape and identify long period variables (LPVs) is described in detail in Appendices A-C in Groenewegen (2004; herafter G04).

Briefly, a first code (see for details Appendix A in G04) sequentially reads in the I-band data for the objects, determines periods through Fourier analysis, fits sine and cosine functions

Send offprint requests to: Martin Groenewegen (groen@ster.kuleuven.ac.be)

^{*} Table 2 is available in electronic form at the CDS via anonymous ftp to cdsarc.u-strasbg.fr (130.79.128.5) or via http://cdsweb.u-strasbg.fr/cgi-bin/qcat?J/A+A/. Figure 1 and Appendices A and B are available in the on-line edition of A&A.

to the light curve through linear least-squares fitting and makes the final correlation with the pre-prepared DENIS and 2MASS source lists. All the relevant output quantities are written to file. This part of the code is adapted significantly to better deal with the specific properties of eclipsing binaries w.r.t. pulsational variables, as described in Appendix A of the present paper. Brief, phase dispersion minimization is used next to Fourier analysis to select the true orbital period, and the EBs candidates are selected based on statistical properties of the phased light curve.

The output file of the first code is read in by the second code (see for details Appendix B in G04). A further selection may be applied (typically on period, amplitude and mean *I*-magnitude), multiple entries are filtered out (i.e. objects that appear in different OGLE fields), and a correlation is made with pre-prepared lists of objects for cross-identification. The output of the second code is a list with EB candidates.

The third step (for details see Appendix C in G04) consists of a visual inspection of the fits to the (phased) light curves of the candidate EBs and a literature study through a correlation with the SIMBAD database. Non-EBs are removed, and sometimes the fitting is redone. The final list of EB candidates is compiled.

4. Results

4.1. Testing the code on selected SMC data

In order to set and finetune the parameters described in Appendix A that define the selection of an EB, and also to demonstrate that with these particular settings EBs can indeed be retrieved, the code is tested and run on the OGLE data of variable stars in the Magellanic Clouds (hereafter MCs; Zebruń et al. 2001).

As the ultimate aim of the project is to define EBs in the GB suitable for distance determinations the parameters that define the selection of EBs (3 statistical parameters that define the shape of the phased lightcurve, and the parameters significance and hifac of the NUMERICAL RECIPES (Press et al. 1992) subroutine fasper) are tuned to retrieve the stars in the lists of "ideal" distance indicators in the SMC previously selected by Udalski et al. (1998) and Wyithe & Wilson (2001) based on the first release of OGLE data (based on a shorter timespan of OGLE data and aperture photometry instead of DIA). What constitutes an "ideal" EB in terms of a distance indicator is difficult to quantify exactly. Typically the system should be well-detached with small values of the stellar radii relative to the semi-major axis $(r/a \lesssim 0.2)$ and have deep eclipses (e.g. Wyithe & Wilson, 2001).

Not all of the stars from Udalski et al. (1998) and Wyithe & Wilson (2001) are listed in the Zebruń et al. (2001) data set. In fact, Wyrzykowski et al. (2004) state that of the 1527 EBs listed by Udalski et al. (1998) only 935 can be found in the DIA catalog of variable stars by Zebruń et al. (2001), and quote the incompleteness of the DIA catalog for faint stars as the probable reason. Of the 153 stars listed by Udalksi et al. (1998) and the 22 unique additional objects in Tables 4 and 5 of Wyithe & Wilson (i.e. not already listed in Udalski et al.), 142 are found

back by Zebruń et al. (2001), and these stars represent the test data set.

Of these 142, 137 are correctly identified as EBs by the program using the parameters mentioned in Appendix A. One object (OGLE005102.88-730941.0) is found with the period as listed by Udalski et al. (1998) but the phased light curve is poor with the DIA data set, and the object is not suitable as a distance indicator from the present data. Two stars would have been correctly identified as EBs were it not that the significance of the peak of the Fourier spectrum is above the adopted threshold. The other two are missed because the parameters that are being used to describe the shape of the phased lightcurve are outliers. At the end of the day, it is deemed acceptable to miss 4 stars out of a 141 suitable candidates. It should be mentioned that these "ideal" distance indicators have orbital periods larger than 0.85 days and so the code is optimised to be sensitive to this period range, and hence will be biased against shorter orbital periods.

4.2. Applying the code to SMC and LMC data

As a further test, the code is applied to the full set of 68 000 lightcurves of variable stars in the SMC and LMC by Zebruń et al. (2001), and compared to the outcome of the previous work by Wyrzykowski et al. (2003, 2004), based on the same dataset as is the present work.

Wyrzykowski et al. (2003) find 2580 EBs in the LMC, and Wyrzykowski et al. (2004) find 1351 EBs in the SMC, based on an artificial neural network. Note that they attempted to find all types of eclipsing binaries, while the aim of the present paper is to detect EBs potentially suitable for distance determination, hence preferentially detached systems.

Applying the code resulted in 1856 LMC and 752 SMC candidate EBs.

For the SMC, 714 of the 752 objects are listed in Wyrzykowski et al. (2004) as EBs. Of the 38 not listed in Wyrzykowski et al., 20 are eliminated at the visual inspection stage as the phased lightcurves are not typical of that of an EB; 13 are in fact known Cepheids. Of the 18 remaining stars, 2 are classified as EB by MOA (Bayne et al. 2002), and 16 are new EBs not previously identified. Names, periods and the phased lightcurve are presented in Appendix B.

For the LMC, 1616 of the 1856 objects are listed in Wyrzykowski et al. (2003) as EBs. Of the 240 not listed in Wyrzykowski et al., 51 are eliminated at the visual inspection stage as the phased lightcurves are not typical of that of an EB; 7 are known Cepheids, 2 are known RR Lyrae and 24 are LPVs. Of the 189 remaining stars, 11 are classified as EB by MACHO (Alcock et al. 1997), and 178 are new EBs not previously identified. Names, periods and the phased lightcurve are presented in Appendix B.

The conclusion is that the simple method developed for detecting EBs is complementary to the neural network method used in Wyrzykowski et al. (2003, 2004) as, considering both MCs, about 7.5% of the detected objects are newly discovered EBs. The number of false candidates (mostly cepheids, RR Lyrae and LPVs) is about 2.5%.

Table 2. First entries in the electronically available table, which lists: OGLE-name, oribital period, and time used to define phase zero.

OGLE name	Period (d)	$T^{(a)}$
bul_sc01_0053	2.521648	530.819
bul_sc01_0108	1.532373	550.789
bul_sc01_0202	4.513265	535.895
bul_sc01_0257	2.378940	540.765
bul_sc01_0422	4.201144	530.836
bul_sc01_0424	1.738786	530.836
bul_sc01_0426	4.236257	530.819
bul_sc01_0487	1.782421	550.789
bul_sc01_0552	2.049995	550.789
bul_sc01_0616	1.761581	530.837
bul_sc01_0691	3.350188	535.895
bul_sc01_0696	1.329869	550.789
bul_sc01_0738	1.427248	540.765
bul_sc01_0777	1.578524	550.789
bul_sc01_0778	1.107325	540.765
bul_sc01_0851	8.904982	550.789

(a) T = (JD-2450000) used to define zero phase in Figure 1. First entries only. Complete table available in electronic form at the CDS.

4.3. Applying the code to the Galactic Bulge

The numerical code is applied to the OGLE-II data in the direction of the Galactic Bulge. After visual inspection of the lightcurves a sample of 3053 objects remain. The largest number of objects that are removed at this stage are LPVs especially at longer periods ($P_{\rm binary} \gtrsim 150$, respectively $P_{\rm pulsation} \gtrsim 75$ days) and EBs with orbital periods $\lesssim 0.85$ days where an alias frequency is picked up, which nevertheless phases well enough to fulfill the initial selection criteria.

The number of objects per field is listed in the last column of Table 1. Table 2 lists the 3053 objects with periods, and Figure 1 displays the phased lightcurves. The typical error in the period is $3\times10^{-4}P$. Only one object is listed in the SIMBAD database, namely bul_sc26_3510 (R.A.= 17h47m28.25s, Dec= -34d46m31.0s), a.k.a. MM5-A V47 in Udalski et al. (1997) and classified as a W UMa-type binary. The period quoted there is 1.10577d while in the present analysis 1.105801d is derived.

5. Summary

The paper presents a simple method to detect eclipsing binaries based on the shape of the phased lightcurve. In view of the ultimate aim to use EBs to derive the distance to the Galactic Centre, the parameters of the model are finetuned to retrieve a large sample of EBs in the SMC previously classified in the literature as potentially suitable for distance determinations. The code is run on the 68 000 OGLE variable stars in LMC and SMC to find 194 apparently previously unclassified EBs, and on the about 222 000 OGLE variable stars in the direction of the Bulge to find about 3000 EBs. It should be stressed that due to the finetuning of the model no short period EBs ($P \lesssim 0.85d$) are among these.

It should also be stressed that altough the code was tuned to retrieve EBs peviously classified in the literature as suitable for distance determinations, the converse is not necesarily true: The objects returned by the code and listed in Tables 2 and B.1 are not *automatically* suitable as potential distance indicators. For example, none of the 15 objects displayed in Figure B.1 seems suitable for this purpose. In this case this is not surprising as only newly discovered EBs, not in the exhaustive lists of Wyrzykowski et al. (2003, 2004), are listed and so these objects have relatively low S/N lightcurves. Of the lightcurves displayed in Figure 1 only a few appear suitable for follow-up studies.

In the future it is planned to select a small sub-sample among the 3000 objects based on a proper analysis of the lightcurve in terms of radii determination and eclipse depth and obtain multi-epoch spectroscopic data in order to derive the fundamental parameters (mass, radius, effective temperature, metallicity) and distance.

Acknowledgements. This research has made use of the SIMBAD database, operated at CDS, Strasbourg, France.

References

Alcock C., Allsman R.A., Alves D., et al., 1997, AJ 114, 326
Andersen J., 1991, A&AR 3, 91
Bayne G., Tobin W., Pritchard J.D., et al., 2002, MNRAS 331, 609
Clausen J.V., 2004, NewAR 48, 679
Grison P., Beaulieu J.-P., Pritchard J.D., et al, 1995, A&AS 109, 447
Groenewegen M.A.T., 2004, A&A 425, 595 (G04)
Groenewegen M.A.T., Blommaert J.A.D.L., 2005, A&A submitted
Guinan E.F., Fitzpatrick E.L., DeWarf L.E., et al., 1998, ApJ 509, L21
Hilditch R.W., Howarth I.D., Harries T.J., 2005, MNRAS 357, 304
Nikolaev S., Drake A.J., Keller S.C., et al., 2003, ApJ 601, 260
Popowski P., Cook K.H., Becker A.C., 2003, AJ 126, 2910
Press W.H., Teukolsky S.A., Vetterling W.T., Flannery B.P., 1992,

Sandage A., Tammann G.A., Reindl B., 2004, A&A 424, 43
Schultheis M., Ganesh S., Simin G., et al., 1999, A&A 349, L69
Stellingwerf R.F., 1978, ApJ 224, 953
Sumi T., 2004, MNRAS 349, 193
Udalski A., Kubiak M., Szymański M., et al., 1994, AcA 44, 317
Udalski A., Szymański M., Kaluzny J., et al., 1995a, AcA 45, 1
Udalski A., Olech A., Szymański M., et al., 1995b, AcA 45, 433
Udalski A., Olech A., Szymański M., et al., 1996, AcA 46, 51
Udalski A., Olech A., Szymański M., et al., 1997, AcA 47, 1
Udalski A., Soszyński I., Szymański M., et al., 1998, AcA 48, 563
Udalski A., Szymański M., Kubiak M. et al., 2002, AcA 52, 217
Wozniak P.R., Udalski A., Szymanski M., et al., 2002 AcA 52, 129
Wyrzykowski L., Udalski A., Kubiak M., et al., 2003, AcA 53, 1
Wyrzykowski L., Udalski A., Kubiak M., et al., 2004, AcA 54, 1
Wyithe J.S.B., Wilson R.E., 2001, ApJ 559, 260

Zebruń K., Soszyński I., Woźniak P., et al., 2001, AcA 51, 317

"Numerical Recipes in Fortran 77", Cambridge U.P.

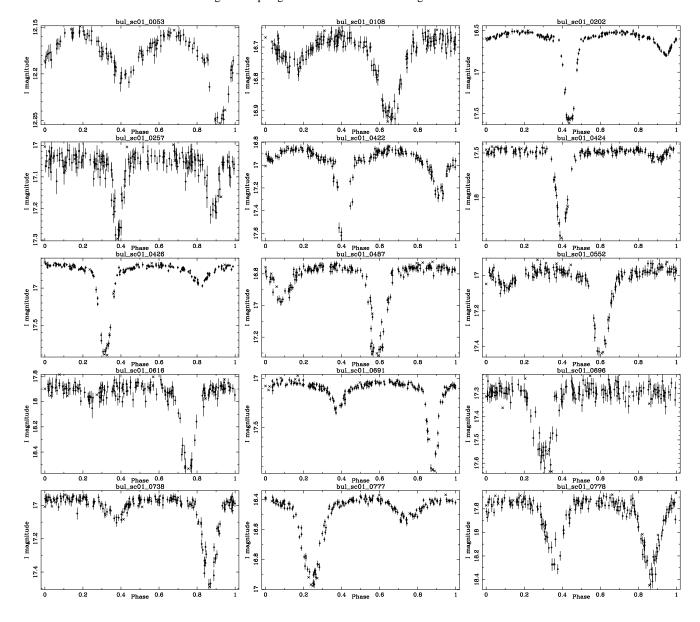


Fig. 1. First 15 entries of the electronically available figure with all phased lightcurves of EBs in the direction of the Galactic Bulge. Crosses indicate data points not included in the analysis. Phase zero is given by the Julian Date listed in Table 2.

Appendix A: The model

Compared to the code described in G04 the part of fitting sine and cosine functions to the lightcurves is omitted as the shape of the lightcurve of an EB is not described by such a functional form.

The determination of the period is done in two steps: using Fourier analysis (as in G04), and subsequently phase dispersion minimization (PDM), as described by Stellingwerf (1978), and which is new to the code.

The Fourier analysis is done with the NUMERICAL RECIPES (Press et al. 1992) subroutine *fasper*. Inputs to it are the time and magnitude arrays. In addition one has to specify two parameters, *ofac* and *hifac*, that indicate a "typical oversampling factor" and the maximum frequency in terms of a "typical" Nyquist frequency.

In the present work *ofac* = 22 (as in G04) and hifac = 21.0 are used (compared to 0.8 in G04). The latter parameter is the determining factor in both the computational speed, and the shortest period that can be found. In this case, it is set to correctly identify the main period in OGLE sc8/119647 (OGLE005938.46-730002.2) with a known orbital period of 0.85494 days (Wyithe & Wilson 2001), which is the shortest period in the test dataset described in the main text. It implies that in the configuration used in the present paper there is a bias in the detection of orbital periods shorter than about 0.85 days, of no severe consequence as the focus is finding detached EBs.

The outputs of *fasper* are the frequency where the peak of the power spectrum occurs and a number indicating a *significance*. One of the main parameters in the code is to provide the critical cut-off above which a period is not considered to be significant. In the present work $significance = 2.2 \times 10^{-5}$ is used, and this is determined empirically, by using the set of detached EBs which the code should be able to retrieve (see below).

As had already been noted in G04 and Groenewegen & Blommaert (2005) in analysing LPVs, the frequency returned from the Fourier analysis in some cases turns out to be a harmonic rather than the true period and this needs then manual refitting of the lightcurve. The same turns out to be the case when the test data set of EBs was initially being analysed. Therefore it was decided to perform a PDM analysis at selected frequencies to decrease manual intervention and hence to allow for a more fully automatic analysis. The θ -statistics as defined by Stellingwerf (1978) is first calculated at the frequency ω , being the frequency of the peak of the power spectrum returned by fasper divided by 2, as the orbital period should normally be twice the period returned from the Fourier analysis because of the primary and secondary eclipse within one orbital period. Then the θ quantity is calculated for frequencies 0.4ω , 0.5ω and $\frac{2}{3}\omega$ and the frequency resulting in the lowest θ -under the condition that it should be smaller than $0.93\theta(\omega)$ is taken as the true orbital frequency. These numbers have been derived from analysis of the objects where the Fourier analysis returned the incorrect orbital period.

The lightcurve is phased with the supposed orbital frequency and from its properties to be described below the candidate EBs are then selected (see Fig A.1 for an example).

A first limit is set at $m_{\rm lim1} = m_{\rm max} - 0.2$ ($m_{\rm max} - m_{\rm min}$), where $m_{\rm max}$ and $m_{\rm min}$ represent the faintest and brightest magnitude¹. If there are less than 10 datapoints fainter than $m_{\rm lim1}$ then it is brightened in steps of 0.04 magnitude until there are.

Then, for a grid of phases ϕ_n (N phase steps of 0.01) it is counted how many of the points fainter than $m_{\mathrm{lim}1}$ are within 0.05 in phase of ϕ_n . The average of this number over the N phase bins defines a "background" level bkg, and the phase where his number is largest– n_{max} -is recorded, ϕ_{max} .

A second limit is set at $m_{\rm lim2}=m_{\rm lim1}-0.2$. From all, n_2 , phase points fainter than $m_{\rm lim2}$ and within 0.2 in phase of $\phi_{\rm max}$, a second parameter rms is determined as the rms of the phase difference between $\phi_{\rm max}$ and the phase of the n_2 data points. A third parameter rat is defined as $n_2/n_{\rm max}$.

An object is classified as an EB candidate if:

- $-n_2/bkg > 4.91$ and rms < 0.0373 and rat < 2.01, or
- $-n_2/bkg > 5.45$ and rms < 0.036, or
- $-n_2/bkg > 5.50$ and rat < 1.64, or
- rms < 0.022 and rat < 2.34.

The principal idea behind this procedure is that compared to the phased light curve of a pulsational variable the one of an EB has at least one minimum, and that the spread in phase at this minimum is limited, and that this also holds at the second magnitude limit (because of the limited width of the eclipse).

The exact value of the parameters have been derived from analysis of a test data set, as described in the main text, and with that setting the program correctly selected 137 out of a 141 objects (= 97%).

Appendix B: Newly discovered EBs in the MCs

This appendix lists the names and periods (Table B.1) and phased lightcureves (Figure B.1) of the newly identified EBs in the SMC and LMC.

Note that like in G04 the 3 brightest data points and the 5% of the data with the largest photometric error bars are automatically rejected.

Table 1. Properties of the OGLE-fields and the number of detected EBs

BUL_SC	l	b	Total ^(a)	Variable ^(b)	$A_{\mathrm{V}}^{(c)}$	EBs ^(d)
1	1.00	2.62	730	4507	1 69 / 1 40	77
1 2	1.08 2.23	-3.62 -3.46	803	4597 5279	1.68 / 1.49 1.55 / 1.65	77 70
3	0.11	-1.93	806	8393	2.89	130
4	0.11	-2.01	774	9096	2.59 / 2.94	146
5	-0.23	-1.33	434	7257	5.73 / - / 4.13	39
6	-0.25	-5.70	514	3211	1.37	41
7	-0.14	-5.91	463	1618	1.33 / 1.28	21
8	10.48	-3.78	402	2331	2.14	29
9	10.59	-3.98	330	1847	2.08	18
10	9.64	-3.44	458	2499	2.23	36
11	9.74	-3.64	426	2256	2.27	25
12	7.80	-3.37	535	3476	2.29 / 2.20	36
13	7.91	-3.58	570	3084	2.06 / 1.82	41
14	5.23	2.81	619	4051	2.49	83
15	5.38	2.63	601	3853	2.77	41
16	5.10	-3.29	700	4802	2.15 / 2.23	48
17	5.28	-3.45	687	4690	1.94 / 2.29	46
18	3.97	-3.14	749	5805	1.83	78
19	4.08	-3.35	732	5255	2.74	61
20	1.68	-2.47	785	5910	1.94 / 2.02	119
21	1.80	-2.66	883	7449	1.83 / 1.78	116
22	-0.26	-2.95	715	5589	2.74	91
23	-0.50	-3.36	723	4815	2.70	68
24	-2.44	-3.36	612	4304	2.52	68
25	-2.32	-3.56	622	3046	2.34	77
26	-4.90	-3.37	728	4713	1.86	76
27	-4.92	-3.65	691	3691	1.69	66
28	-6.76	-4.43	406	1472	1.64	26
29	-6.64	-4.62	492	2398	1.53	44
30	1.94	-2.84	762	6893	1.91 / 1.78	137
31	2.23	-2.94	790	4789	1.81 / 1.74	87
32	2.34	-3.14	797	5007	1.61 / 1.82	99
33	2.35	-3.66	739	4590	1.70 / 1.82	44
34	1.35	-2.40	961	7953	2.52 / 2.32	127
35	3.05	-3.00	771	5169	1.84 / 2.20	64
36	3.16	-3.20	873	8805	1.62 / 1.52	85
37	0.00	-1.74	664	8367	3.77	119
38	0.97	-3.42	710	5072	1.83 / 1.94	119
39	0.53	-2.21	784	7338	2.63 / 2.70	144
40	-2.99	-3.14	631	4079	2.94	48
41	-2.78	-3.27	603	4035	2.65	55
42	4.48	-3.38	601	4360	2.29	67
43	0.37	2.95	474	3351	3.67	34
44	-0.43	-1.19	319	7836	6.0 / - / 6.00	32
45	0.98	-3.94	627 552	2262	1.64 / 1.53	4
46	1.09	-4.14	552	2057	1.71 / 1.65	3
47	-11.19	-2.60	301	1152	2.60	7
48	-11.07	-2.78	287	973 826	2.35	9
49 total	-11.36	-3.25	251 30490	826 221701	2.09	6 3053
(a) Total number of objects detected in the field. From Udalski et al. (2002), in units						

⁽a) Total number of objects detected in the field. From Udalski et al. (2002), in units of 10³ objects

⁽b) Total number of candidate variable stars. From Wozniak et al. (2002).

⁽c) Visual extinction. From Sumi (2004), except for SC44, where $A_V = 6.0$ has been adopted based on the proximity to SC5. The second value—when listed—comes from Popowski et al. (2003). The third value—when listed—comes from Schultheis et al. (1999).

⁽d) Total number of EBs.

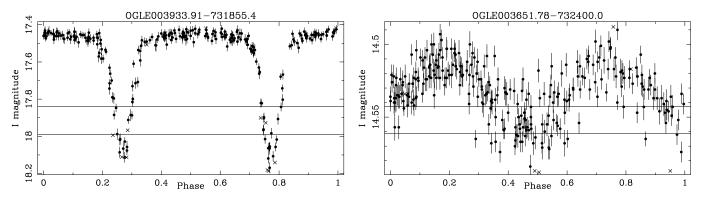


Fig. A.1. Example of a phased lightcurve of an EB (left) and an LPV (right), and the two magnitude limits discussed in the text. The identification of an EB is based on the number and statistical properties of the data points fainter than these two limits.

Table B.1. Properties of newly discovered EBs in the MCs.

Field	OGLE name	Period (d)	$T^{(a)}$
smc_sc1	OGLE003708.38-734304.6	8.720979	627.870
smc_sc3	OGLE004445.50-725934.5	204.406036	625.927
smc_sc3	OGLE004518.23-731522.7	1.002808	621.836
smc_sc4	OGLE004818.07-730722.6	3.867470	622.874
smc_sc5	OGLE004932.55-731621.1	2.611493	466.548
smc_sc5	OGLE005003.11-730854.6	197.654480	466.548
smc_sc5	OGLE005035.13-732305.5	3.332872	466.548
smc_sc6	OGLE005138.20-730047.2	6.514974	466.571
smc_sc6	OGLE005140.20-731532.5	91.864151	466.571
smc_sc6	OGLE005205.17-731609.1	256.679626	466.571
smc_sc6	OGLE005207.25-724626.8	1.763637	466.571
smc_sc6	OGLE005245.82-732210.0	2.961430	466.571
smc_sc6	OGLE005353.43-724018.8	2.950854	466.571
smc_sc7	OGLE005617.71-723905.9	1.554488	626.927
smc_sc8	OGLE005849.12-730041.9	1.424265	626.935
smc_sc10	OGLE010521.71-723740.0	136.450470	621.867
lmc_sc15	OGLE050100.28-692243.8	1.125093	726.815
lmc_sc15	OGLE050100.36-690534.7	27.095217	726.815
lmc_sc15	OGLE050124.20-683728.9	4.690511	726.815
lmc_sc15	OGLE050124.33-690033.6	5.216741	726.815
lmc_sc15	OGLE050129.81-683647.0	5.018933	726.815
lmc_sc14	OGLE050301.95-685526.9	9.183692	726.806
lmc_sc14	OGLE050337.43-685622.7	1.512742	726.806
lmc_sc14	OGLE050415.35-692123.5	3.679661	726.806
lmc_sc14	OGLE050428.68-685525.7	29.598274	726.806
lmc_sc14	OGLE050438.66-685410.7	2.435237	726.806
lmc_sc14	OGLE050440.04-692235.7	1.161064	726.806
lmc_sc13	OGLE050505.98-690310.0	1.048826	726.798
lmc_sc13	OGLE050511.85-685947.9	3.438104	726.798

(a) T = (JD-2450000) used to define zero phase in Figure B.1.

First entries only. Complete table available in electronic form at the CDS.

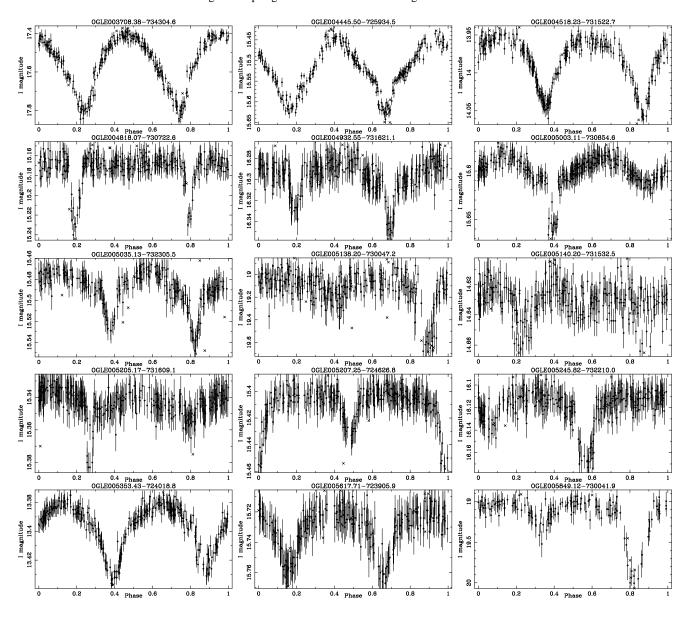


Fig. B.1. First entries of electronically available figure with the phased lightcurves of newly discovered EBs in the MCs. Phase zero is given by the Julian Date listed in Table B.1.